

CONTROL SCHEME FOR VOLTAGE REGULATION IN MICRO GRIDS TO ENSURE MAXIMUM POWER POINT TRACKING (MPPT)

Mr. K. CHANDRA SEKHAR, Mr. T. SIVARAM

Assistant Professor, Department of Electrical & Electronics Engineering, Malla Reddy Engineering College and Management Sciences, Kistapur, Medchal(Dt); T.S, India

ABSTRACT

This paper presents a sliding mode controller to address the problem of voltage regulation in micro grids involving doubly fed induction wind generators (DFIGs). The control objective is to achieve terminal voltage regulation while ensuring maximum power point tracking (MPPT). The control development is based on voltage sensitivity analysis to eliminate the possibility of interference with the other voltage regulation devices in the micro grid. The proposed method: 1) does not require synchronous coordinate transformation, 2) eliminates the need for decoupled proportional-integral (PI) loops, and 3) is local and can be implemented in the absence of widespread communication systems or remote measurements. Additionally, its control performance is not degraded by errors in system parameters. The performance of the method is illustrated on the IEEE 13-bus distribution network. Dynamic models are considered for the DFIG, converters, and internal controllers along with their operational limits. Stochastic Fluctuations in wind speed are modeled with NREL Turbid while accounting for the tower shadow and wind shear. Dynamic simulations (in PSCAD/EMTDC) are presented to assess the control performance with voltage Fluctuation compensation and control system robustness.

KEYWORDS: *doubly fed induction generator (DFIG), direct power control, micro grid, robust sliding mode control, voltage regulation.*

INTRODUCTION

AMICROGRID is a part of a distribution network with at least one distributed energy source which can operate in-dependently as an island when necessary [1]. Doubly fed induction generator(DFIG)-based wind generation is an attractive option for sustainable energy integration in micro grids. In micro-grids with significant wind energy penetration, wind speed variations translate to fluctuations in electrical variables and con-tributes towards power quality issues [2], [3] such as variations in bus voltages [4], [5]. As noted in IEEE 1547, such fluctuations can disrupt the normal operation of voltage regulation de-vices; therefore, the coupling of a controllable reactive power source with the wind energy system is proposed to flatten out the voltage variations [6]. Since direct voltage regulation by wind energy systems may interfere with other voltage regulation de-vices, it is prohibited by IEEE 1547. A suitable method of re-active power management of DFIG wind systems based on the voltage sensitivity analysis is proposed in [7].

The method eliminates the potential for interference with other voltage regulation devices by locally adjusting the DFIG reactive power based on voltage sensitivity analysis. However, the method in [7] is based on the classical control and performed by the decoupled PI rotor current control loops. Hence the control performance is highly dependent on PI controller parameters and DFIG parameters [8], which are subject to unavoidable errors. Since inaccurate parameters degrade control performance, direct torque control (DTC) and direct power control(DPC)methods based on the sliding mode control (SMC) have been proposed as appropriate alternatives [9], [10].Reference [11]presents a DTC method based on the estimation of ,and[8]utilizes estimated stator to avoid difficulties associated with the

rotor flux estimation. SMC-based DTC methods are proposed in [12] and [13] while special consideration is spent on the wind turbine mechanical stress. The method proposed by [12] improves the wind system reliability, and the method in [13] governs the wind turbine in different operation regions. Reference [14] achieves constant switching frequency for the SMC-based DPC. In [15], and SMC strategy is taken into account which includes continuous and discontinuous parts and guarantees the maximum power point tracking (MPPT) and least copper losses of a doubly fed reluctance generator. Reference [16] proposes a high order SMC-based DTC for marine DFIG wind turbines and [10] eliminates the need of rotor speed adaption in the DTC methods by using a sliding mode observer.

This paper proposes a sliding mode controller to realize the objective of terminal voltage regulation in DFIG-based micro-grids. The control principle is developed based on voltage sensitivity analysis proposed in [7]. The proposed controller employs a sliding mode controller which does not require synchronous coordinate transformations. The method eliminates the need for decoupled PI control loops and thus control performance is not degraded by the inaccuracies in the system parameters. The method is local and can be implemented in the absence of communication system without any interference with the other voltage regulation devices in the micro grid. The performance of the method is illustrated on the IEEE 13-bus distribution network [17].

Stochastic Fluctuations in wind speed are modeled with NREL Turbid while accounting for the tower shadow and wind shear. Dynamic simulations (in PSCAD/EMTDC) are presented to assess the control performance with voltage fluctuation compensation and control system robustness. The rest of the paper is organized as follows. The system structure and assumptions are described in Section II. The voltage sensitivity analysis and the method of choosing target bus are discussed in Section III. Dynamic behavior of DFIG and robust SMC design are analyzed in Sections IV and V, respectively, followed by the simulation results in Section VI. The conclusions are noted in Section VII.

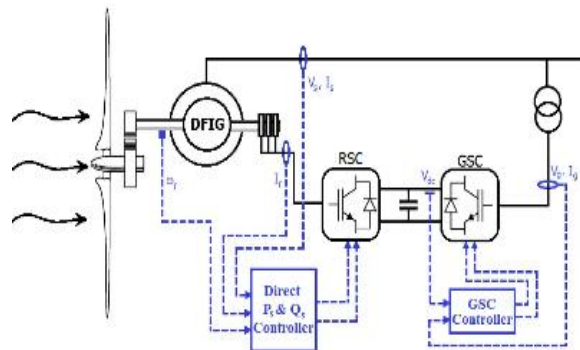


Fig. 1. Schematic diagram of a DFIG

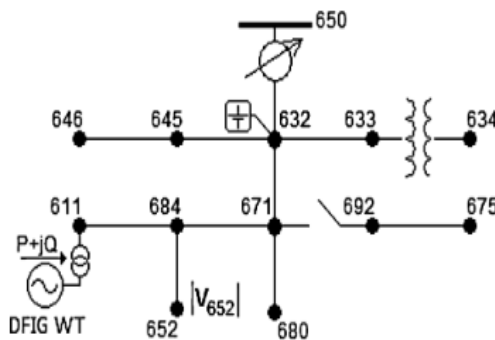


Fig. 2. Schematic diagram of the modeled IEEE 13-bus system

SYSTEM STRUCTURE

A schematic diagram of a DFIG-based wind energy generation System is shown in Fig.1. The system employs two back-to-back Converters a rotor side converter (RSC) and a grid side converter (GSC). Typically, these converters are rated at about 25%–30 of the generator rating. While the RSC is used to adjust the rotor current, the GSC is responsible to maintain the dc link voltage. Together, the converters are able to control reactive power exchanges with the network. Two DFIGs (each rated at 2.2 MW) are connected to bus 611 of the IEEE 13-bus distribution network as shown in Fig. 2.

The network is connected to the bulk power system through bus 650, with a short circuit capacity of 58.52 MVA and X/R ratio of 1/4. It is further assumed that: 1) the two DFIG systems at bus 611 are identical; 2) the DFIG converters employ pulse wide modulation (PWM); 3) distribution lines include resistive and inductive characteristics; 4) wind speed fluctuations, aerodynamics of the turbine, wind shear, and tower shadow lead to fluctuations in active power, and consequently the voltage; 5) the system is three-phase balanced. In the simulations, the PSCAD/EMTDC wound rotor induction generator model is used to represent a DFIG. The model of aerodynamics, including wind and wind turbine models, are discussed in the rest of this section

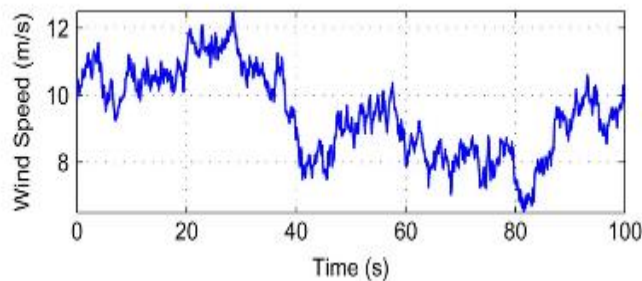


Fig. 3. Equivalent wind speed produced by Turbsim

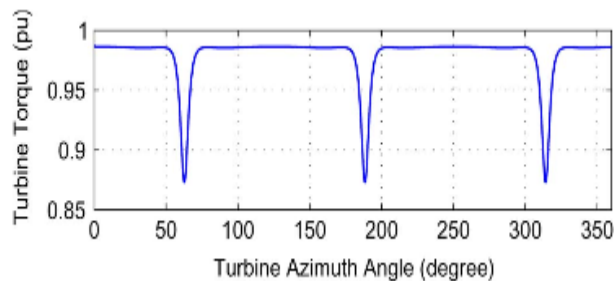


Fig. 4. Tower shadow and wind shear effects on the turbine torque

A. Aerodynamics Model

Turbid is a precise wind model developed by the National Renewable Energy Laboratory (NREL). It is a turbulent wind simulator that has been developed for simulation of a full field for turbulence structures [18]. An ample of wind speed produced by Turbid for 100 s is shown in Fig. 3.

A simplified aerodynamic model is normally used when the Electrical behavior of the wind turbine is the main interest of Study, but wind shear and tower shadow phenomena influence the output voltage [4], [5]. The term wind shear is used to describe the variation of wind speed with height, and the term tower shadow describes the redirection of wind due to the tower structure. In three-bladed turbines, power pulsations occur at what is known as 3p frequency, and it is the same frequency at which blades pass by the tower. In [19], the fatigue, aerodynamics, structures, and turbulence (FAST) package is proposed to model the wind turbine while considering a complex flexible structure based infinite-element methods [20]. Reference [21] neglects the tower shadow and wind shear for large

wind farms, but for single turbine it suggests the addition of 3p pulsations to the turbine mechanical torque.

A suitable model of 3p pulsations is developed by [22]. The model computes torque variations for a three-bladed turbine including the effects of wind shear and tower shadow. The output torque computed with this model (turbine parameters in Appendix) is shown in Fig. 4 from which one can note the drop in output torque three times per revolution.

VOLTAGE REGULATION BASED ON THE VOLTAGE SENSITIVITY ANALYSIS

The control concept for voltage regulation based on voltage sensitivity analysis appears in [7]. However, it is briefly de-scribed here to make the presentation self-contained. The power flow equations for the system considering both inductive and resistive characteristics of the power lines are

$$\begin{cases} P_k = \sum_{n=1}^N |V_k| \cdot |V_n| \cdot |Y_{kn}| \cdot \cos(\theta_{kn} + \delta_n - \delta_k) \\ Q_k = \sum_{n=1}^N |V_k| \cdot |V_n| \cdot |Y_{kn}| \cdot \sin(\theta_{kn} + \delta_n - \delta_k) \end{cases} \quad (1)$$

where P_k and Q_k are the active and reactive powers of bus k , $Y_{kn} \angle \theta$ is the admittance of the line from bus k to bus n , and $V_n \angle \delta_n$ is the voltage at bus n . Assuming the swing bus voltage is constant, any variation in the network power flow inside the network affects the bus voltages.

$$\begin{vmatrix} \Delta P \\ \Delta Q \end{vmatrix} = \begin{vmatrix} \frac{\partial P}{\partial \delta} & \frac{\partial P}{\partial V} \\ \frac{\partial Q}{\partial \delta} & \frac{\partial Q}{\partial V} \end{vmatrix} \cdot \begin{vmatrix} \Delta \delta \\ \Delta V \end{vmatrix} \quad (2)$$

The sensitivity of the bus voltages to deviations in active/re-active powers is obtained by computing the power flow Jacobean linearizing the power flow equations about an operating point given by. Provided the Jacobian is well conditioned, deviations in bus Voltage magnitudes can be obtained from

$$\begin{vmatrix} \Delta \delta \\ \Delta V \end{vmatrix} = \begin{vmatrix} [S_{\delta p}] & [S_{\delta q}] \\ [S_{vp}] & [S_{vq}] \end{vmatrix} \cdot \begin{vmatrix} \Delta P \\ \Delta Q \end{vmatrix} \quad (3)$$

where $S_{\delta p}$ and $S_{\delta q}$ are the sensitivities of the bus angles to the active and reactive powers, respectively, and S_{vp} and S_{vq} are the sensitivities of the bus voltage magnitudes.

Denote the wind generator bus by “ w ” and the target bus (where voltage regulation is sought) by “ v .” From (3), the voltage variations at bus “ v ” due to active/reactive power variations at “ w ” are given by

$$\Delta V_v = S_{vp_{vw}} \cdot \Delta P_w + S_{vq_{vw}} \cdot \Delta Q_w \quad (4)$$

$$\Delta V_v = 0 \Rightarrow \frac{\Delta Q_w}{\Delta P_w} = \frac{Q - Q_0}{P - P_0} = -\frac{S_{vp_{vw}}}{S_{vq_{vw}}} \quad (5)$$

Where (P,Q) correspond to the operating condition. Consequently, the required reactive power adjustments to compensate for voltage fluctuations due to active power variations are given by

$$Q_w = -\frac{Svp_{vw}}{Svq_{vw}}(P_w - P_0) + Q_0. \quad (6)$$

$$PF_w = \frac{|Svq_{vw}|}{\sqrt{Svp_{vw}^2 + Svq_{vw}^2}} \quad (7)$$

Where p is the power factor of the wind generator (bus).Producing large amounts of reactive power by wind generator increases its winding currents and relevant losses. To improve the efficiency of the wind generator operation, set point may be chosen such that, where is the average active power of the wind generator.

A. Choice of Sensitive Voltage Bus(es)

The method presented in the previous section achieves voltage regulation at a single target bus. This can be generalized so that the control is exercised to extend voltage regulation at multiple buses. This is done as follows. Consider a group of buses. Denote an by the weight, or importance ascribed to bus. Then the objective of voltage regulation at multiple buses can be met by setting

$$\sum_{i=1}^n w_i (Svp_{iw} + K_Q \cdot Svq_{iw})^2 = 0. \quad (8)$$

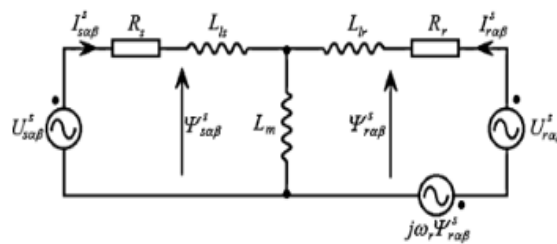


Fig. 5. Equivalent circuit of a DFIG in the stator stationary reference frame.

Thus, K_Q , the best ratio of reactive to active powers of the wind generator, can be determined from (8). A sliding mode controller to implement (6) is developed in Section V following the dynamic model development explained as follows in Section IV.

DYNAMIC BEHAVIOR OF DFIG IN THE STATOR STATIONARY REFERENCE FRAME

Fig. 5 displays the equivalent circuit of a DFIG in the stator stationary reference frame where the flux linkage vectors are given by

$$\begin{aligned} \psi_{s\alpha\beta}^s &= L_s I_{s\alpha\beta}^s + L_m I_{r\alpha\beta}^s \\ \psi_{r\alpha\beta}^s &= L_m I_{s\alpha\beta}^s + L_r I_{r\alpha\beta}^s. \end{aligned} \quad (9)$$

From Fig. 5, stator and rotor voltage vectors in the Stator stationary reference frame are as follows:

$$\begin{aligned} U_{s\alpha\beta}^s &= R_s I_{s\alpha\beta}^s + \frac{d\psi_{s\alpha\beta}^s}{dt} \\ U_{r\alpha\beta}^s &= R_r I_{r\alpha\beta}^s + \frac{d\psi_{r\alpha\beta}^s}{dt} - j\omega_r \psi_{r\alpha\beta}^s \end{aligned} \quad (10)$$

as the system disturbance and uncertainties, the dynamics of the DFIG-based system are given by

$$\dot{\mathbf{x}} = f(\mathbf{x}) + B \cdot \mathbf{u} + \delta \quad (11)$$

where the relevant terms are given by

$$\begin{aligned} f_1(\mathbf{x}) &= \frac{1}{D} \cdot (-R_s L_r i_{s\alpha}^s + L_m^2 \omega_r i_{s\beta}^s + R_r L_m i_{r\alpha}^s \\ &\quad + L_m L_r \omega_r i_{r\beta}^s + L_r u_{s\alpha}^s) \\ f_2(\mathbf{x}) &= \frac{1}{D} \cdot (L_m^2 \omega_r i_{s\alpha}^s + R_s L_r i_{s\beta}^s + L_m L_r \omega_r i_{r\alpha}^s \\ &\quad - R_r L_m i_{r\beta}^s - L_r u_{s\beta}^s) \\ f_3(\mathbf{x}) &= \frac{1}{D} \cdot (R_s L_m i_{s\alpha}^s - L_m L_s \omega_r i_{s\beta}^s - R_r L_s i_{r\alpha}^s \\ &\quad - L_r L_s \omega_r i_{r\beta}^s - L_m u_{s\alpha}^s) \\ f_4(\mathbf{x}) &= \frac{1}{D} \cdot (+L_m L_s \omega_r i_{s\alpha}^s + R_s L_m i_{s\beta}^s + L_r L_s \omega_r i_{r\alpha}^s \\ &\quad - R_r L_s i_{r\beta}^s - L_m u_{s\beta}^s) \\ f_5(\mathbf{x}) &= \frac{P}{H} \cdot \left(T_m - \frac{3PL_m}{4D} \cdot (i_{s\alpha}^s i_{r\beta}^s - i_{s\beta}^s i_{r\alpha}^s) \right) \end{aligned} \quad (12)$$

And

$$B = \frac{1}{D} \cdot \begin{bmatrix} -L_m & 0 \\ 0 & -L_m \\ L_s & 0 \\ 0 & L_s \\ 0 & 0 \end{bmatrix} \quad (13)$$

$$\begin{aligned} P_s &= -\frac{3}{2} (i_{s\alpha}^s u_{s\alpha}^s + i_{s\beta}^s u_{s\beta}^s) \\ Q_s &= -\frac{3}{2} (i_{s\alpha}^s u_{s\beta}^s - i_{s\beta}^s u_{s\alpha}^s). \end{aligned} \quad (14)$$

ROBUST SLIDING MODE CONTROL DESIGN

The basic idea in sliding mode control (SMC) is to steer the system's state trajectory into a user defined surface and maintain the state on that surface for subsequent time. This surface, known as the switching surface, defines the control law. The system trajectory is governed by the sliding surface and the control law can be adapted to compensate for parametric variations or structured uncertainties inherent in models [23], [9]. Here, the sliding surface is chosen to obtain voltage regulation [via reactive power production based on (6)] while ensuring MPPT. Therefore, two sliding variables are defined namely: a) MPPT sliding variable; and b) reactive power control sliding variable. This section discusses the sliding surface and design in detail. For further details on SMC, the reader is encouraged to consult [24] and [25]

A. MPPT Sliding Variable

The primary objective of the control system is performing the MPPT to capture the most possible energy from wind. Temporarily neglecting tower shadow and wind shear effects, the turbine optimal torque and turbine optimum angular speed are given by [7]

$$T_{opt} \approx \rho AV^2 R \frac{C_{\rho max}}{\lambda_{opt}}$$

$$\omega_{opt} = \frac{\lambda_{opt} V}{R} \quad (15)$$

$$P_m^* = T_{opt} \omega_{opt}. \quad (16)$$

Based on (16) and considering the DFIG losses, stator output power references calculated and the lookup table is prepared. Thirst sliding variable should enforce the generator output power to follow and hence expressed by

$$s_1(\mathbf{x}) = P_s^* - P_s = P_s^* + \frac{3}{2} (i_{s\alpha}^s u_{s\alpha}^s + i_{s\beta}^s u_{s\beta}^s). \quad (17)$$

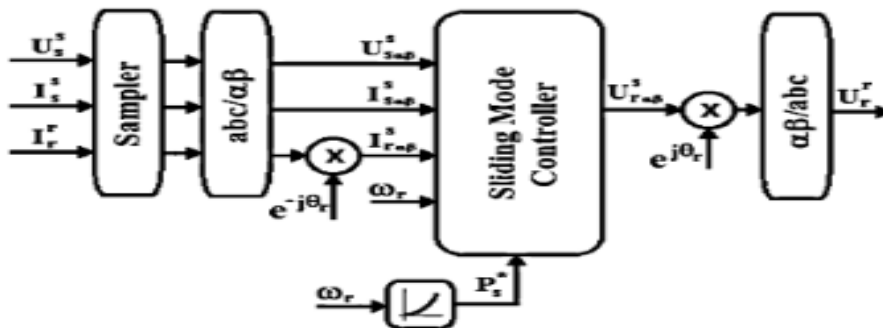


Fig. 6. Schematic diagram of the robust MIMO controller

B. Reactive Power Control Sliding Variable

To ensure the minimum effect of the wind power on the target bus voltage, the second sliding variable is expressed as follows:

$$s_2(\mathbf{x}) = K_Q \cdot P_s - Q_s \quad (18)$$

$$s_2(\mathbf{x}) = K_Q \cdot (P_s - P_0) - Q_s. \quad (19)$$

C. Robust MIMO Sliding Mode Controller

A control system based on the defined sliding manifold should enforce the states of the system to reach the manifold intersection and keeps them there. With as a Lyapunov function candidate, the control design includes three steps: a) system dynamic drift cancellation, b) manifold intersection reaching, and c) control system robustness [15] as follows:

$$\mathbf{u}(\mathbf{x}) = \mathbf{u}_a(\mathbf{x}) + \mathbf{u}_b(\mathbf{x}) + \mathbf{u}_c(\mathbf{x}). \quad (20)$$

It should be noted that the final output of the controllers limited by a saturation function to keep it within the accept-able range. A schematic diagram of the controller is shown in Fig. 6 and the design of each term is discussed in the rest of this section

1) Design of, Drift Cancellation The reason for the first control term is the system dynamic drift cancellation. Assume the system has reached the intersection manifold and there is no disturbance, therefore, variables of Lyapunov function should remain unchanged

,i.e.

$$W' = S \cdot \frac{\partial S}{\partial \mathbf{x}} \cdot \mathbf{x}' = 0. \quad (21)$$

$$\frac{\partial S}{\partial \mathbf{x}} \cdot [f(\mathbf{x}) + B \cdot \mathbf{u}_a(\mathbf{x})] = 0 \quad (22)$$

$$\mathbf{u}_a(\mathbf{x}) = - \left(\frac{\partial S}{\partial \mathbf{x}} B \right)^{-1} \cdot \left(\frac{\partial S}{\partial \mathbf{x}} f(\mathbf{x}) \right). \quad (23)$$

Using (12), (13), (17), (18), and (23), $\mathbf{u}_{a\alpha\beta}^s(\mathbf{x})$ is as follows:

$$\mathbf{u}_{a\alpha\beta}^s(\mathbf{x}) = \begin{bmatrix} \frac{D}{L_m} f_1(\mathbf{x}) \\ \frac{D}{L_m} f_2(\mathbf{x}) \end{bmatrix}. \quad (24)$$

2) Design of, Manifold Intersection Reaching:

The second term of the controller enforces the system to reach the manifold intersection. When the system is out of the manifold intersection and there is no disturbance, the time derivative of the Lyapunov function should move toward zero (i.e.,). Several control laws can fulfill, each having different reaching characteristics. References [26] and [27] suggest the convergence speed which is proportional to the distance to the manifold intersections follows:

$$\frac{\partial S}{\partial \mathbf{x}} \cdot [f(\mathbf{x}) + B \cdot (\mathbf{u}_a(\mathbf{x}) + \mathbf{u}_b(\mathbf{x}))] = -\Gamma S \quad (25)$$

$$\mathbf{u}_b(\mathbf{x}) = - \left(\frac{\partial S}{\partial \mathbf{x}} B \right)^{-1} \Gamma S \quad (26)$$

Where Γ is a positive definite matrix. A simple choice for Γ is a positive definite diagonal matrix. Using (12), (13), (17), (18), and (26), the second term of controller is as follows:

$$\mathbf{u}_{b\alpha\beta}^s(\mathbf{x}) = \begin{bmatrix} \frac{2D \left(\gamma_1 s_1 u_{s\alpha}^s + \gamma_2 s_2 u_{s\beta}^s \right)}{3L_m \left(u_{s\alpha}^{s^2} + u_{s\beta}^{s^2} \right)} \\ \frac{2D \left(\gamma_1 s_1 u_{s\beta}^s - \gamma_2 s_2 u_{s\alpha}^s \right)}{3L_m \left(u_{s\alpha}^{s^2} + u_{s\beta}^{s^2} \right)} \end{bmatrix} \quad (27)$$

$$\Gamma = \begin{bmatrix} \gamma_1 & 0 \\ 0 & \gamma_2 \end{bmatrix}, \quad \gamma_1, \gamma_2 > 0. \quad (28)$$

3) Design of, Control System Robustness:

In the presence of disturbance and uncertainty, two terms of system dynamic drift cancellation and manifold intersection reaching are not enough to guarantee the operation of the system on the manifold intersection. Therefore, the third term of the controllers synthesized for the robustness of the system. For bounded disturbances and uncertainties in(11), the Lyapunov function should still move toward zero, i

$$\frac{\partial S}{\partial \mathbf{x}} \cdot [f(\mathbf{x}) + B \cdot (\mathbf{u}_a(\mathbf{x}) + \mathbf{u}_b(\mathbf{x}) + \mathbf{u}_c(\mathbf{x})) + \delta] = -\Gamma S. \quad (29)$$

Since exact value of system disturbances and uncertainties are unknown, the following discontinuous term can be considered [15]:

$$\begin{cases} \mathbf{u}_c(\mathbf{x}) = - \left\{ \frac{\partial S}{\partial \mathbf{x}} B \right\}^{-1} \Lambda \text{sgn}(S) \\ \Lambda = \text{Diag} \cdot \left(\left| \frac{\partial s}{\partial x} \right| \boldsymbol{\delta}_m \right) \end{cases} \quad (30)$$

with equal to the maximum possible disturbance and uncertainty. Hence, using signup function in the design of may cause chattering and result in high heat losses, high-slope satu-ration function may be taken into account [23] as follows

$$\mathbf{u}_c = - \left\{ \frac{\partial S}{\partial \mathbf{x}} B \right\}^{-1} \Lambda \text{sat} \left(\frac{S}{\epsilon} \right) \quad (31)$$

$$\text{sat} \left(\frac{S}{\epsilon} \right) = \begin{cases} \frac{S}{\epsilon} & \left| \frac{S}{\epsilon} \right| \leq 1 \\ \text{sgn} \left(\frac{S}{\epsilon} \right) & \left| \frac{S}{\epsilon} \right| > 1 \end{cases} \quad (32)$$

$$\mathbf{u}_{c\alpha\beta}^s(\mathbf{x}) = \begin{bmatrix} \frac{Du_{s\alpha}^s (\delta_{1m} |u_{s\alpha}^s| + \delta_{2m} |u_{s\beta}^s|)}{L_m (u_{s\alpha}^{s2} + u_{s\beta}^{s2})} \cdot \text{sat} \left(\frac{s_1}{\epsilon} \right) + \dots \\ \frac{Du_{s\beta}^s (\delta_{2m} |u_{s\alpha}^s| + \delta_{1m} |u_{s\beta}^s|)}{L_m (u_{s\alpha}^{s2} + u_{s\beta}^{s2})} \cdot \text{sat} \left(\frac{s_2}{\epsilon} \right) \\ \frac{Du_{s\beta}^s (\delta_{1m} |u_{s\alpha}^s| + \delta_{2m} |u_{s\beta}^s|)}{L_m (u_{s\alpha}^{s2} + u_{s\beta}^{s2})} \cdot \text{sat} \left(\frac{s_1}{\epsilon} \right) + \dots \\ \frac{Du_{s\alpha}^s (\delta_{2m} |u_{s\alpha}^s| + \delta_{1m} |u_{s\beta}^s|)}{L_m (u_{s\alpha}^{s2} + u_{s\beta}^{s2})} \cdot \text{sat} \left(\frac{s_2}{\epsilon} \right) \end{bmatrix} \quad (33)$$

4) Verification of Sliding Mode Operation:

The negativenes of the time derivative of the selected Lyapunov function under the assumptions and conditions in this paper can be verified as follows:

Based on (11) and by using (20), (23), (26), (31), and (34), the time derivative of the Lyapunov function is as follows:

$$W' = S^T \cdot \frac{\delta S}{\delta \mathbf{x}} \cdot \mathbf{x}'. \quad (34)$$

$$W' = -\Gamma S^T S - S^T \Lambda \text{sgn}(S) + S^T \frac{\delta S}{\delta \mathbf{x}} \boldsymbol{\delta}. \quad (35)$$

$$\begin{vmatrix} \frac{\delta S}{\delta \mathbf{x}} \boldsymbol{\delta}_m & \geq & \frac{\delta S}{\delta \mathbf{x}} \boldsymbol{\delta} \\ \Gamma S^T S & \geq & 0 \\ S^T \text{sgn}(S) & \geq & 0 \end{vmatrix} \Rightarrow W' < 0. \quad (36)$$

SIMULATION RESULTS

Simulations are carried out for two DFIG reactive power control modes of:

- 1) UPF: unity power factor operation;
- 2) PCM (proposed control method): based on (6)—voltage regulation at bus 652. For each of the control modes, three different loading conditions is considered:

- 1) Light load condition—50% of the nominal loading;

- 2) Medium load condition—with nominal loads of the IEEE 13-bus distribution network;
- 3) Heavy load condition—150% of nominal loading

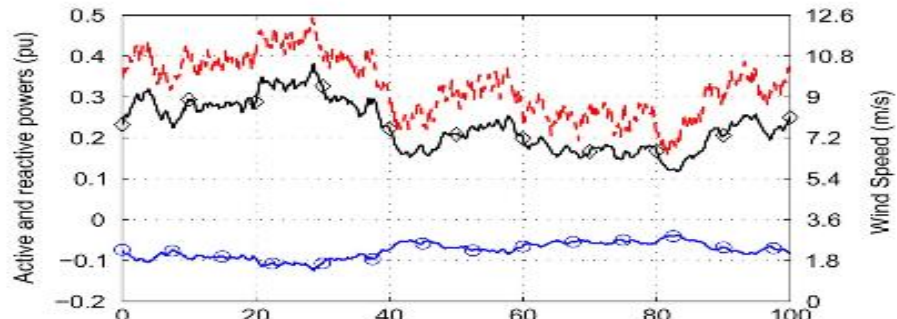


Fig. 7. Active and reactive powers produced by one of the DFIG wind systems with the applied wind speed (dashed)

TABLE 1
MAXIMUM VOLTAGE VARIATIONS IN DIFFERENT CONTROL MODE (%)

Bus Number	Load Condition					
	Low		Med.		High	
	UPF	PCM	UPF	PCM	UPF	PCM
632	2.49	0.05	3.04	0.25	3.65	0.60
633	2.49	0.05	3.04	0.25	3.66	0.60
634	2.51	0.05	3.11	0.25	3.77	0.62
645	2.49	0.05	3.05	0.25	3.66	0.60
646	2.49	0.05	3.05	0.25	3.66	0.60
671	3.40	0.06	4.00	0.28	4.68	0.66
680	3.40	0.06	4.00	0.28	4.68	0.66
675	3.40	0.06	4.01	0.28	4.69	0.66
684	3.90	0.18	4.51	0.48	5.20	0.95
652	3.91	0.18	4.52	0.48	5.20	0.95
611	4.41	0.37	5.02	0.77	5.71	1.31

UPF: Unity power factor operation
PCM: Reactive power control based on (6)

The sensitivity factors in (6) are calculated based on the operation of the micro grid under the nominal load condition. Sensitivity factors of target bus (Bus 652) voltage to the wind bus (bus611) active and reactive power variations are and respectively. Therefore, (7) for voltage regulation of Bus 671 is as follows:

$$PF_w = \frac{0.1759}{\sqrt{0.057^2 + 0.1759^2}} = 0.9513. \quad (37)$$

Different wind speed series are considered with mean wind Speed value from 6 to 11 m/s in 1-m/s steps, and simulations are carried out for 100 s, each of the wind speed series. For example, Fig. 7 displays the active and reactive powers produced by one FIG for the wind speed shown in Fig. 3. The maximum voltage variation (in %) experienced at each of the buses, with various wind speed series, under three loading conditions and with each of the control modes is noted in Table I. For example, at bus652, the proposed control method is effective in significantly reducing the voltage swing (from 4.52% to 0.48%) under the normal load condition. The results are also consistent across all other buses in the system. The corresponding time domain simulations under different net work conditions are presented next and system parameters are noted in the Appendix. The sampling frequency for the control system inputs is 9720 Hz and PWM switching frequency is 2430 Hz

A. Light Load Condition of Microgrid

Fig. 8 displays voltage variations of bus 652 under light load
Conditions of the micro grid when the wind speed shown in Fig. 3

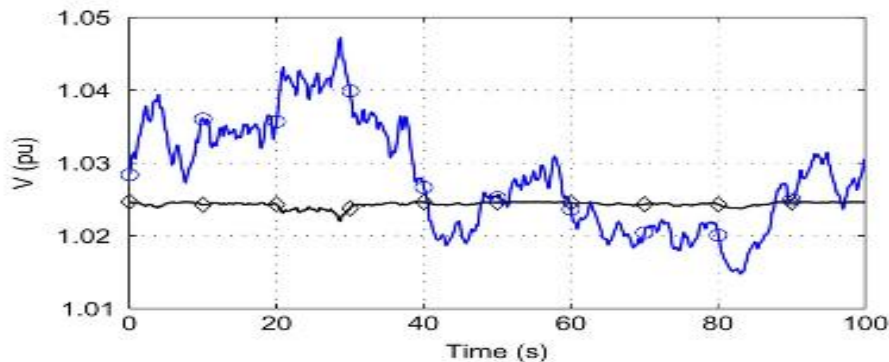


Fig. 8. Voltage at sensitive bus (652) in the grid connected mode under light load conditions. DFIG reactive power regulated by PCM:, and unity power factor operation

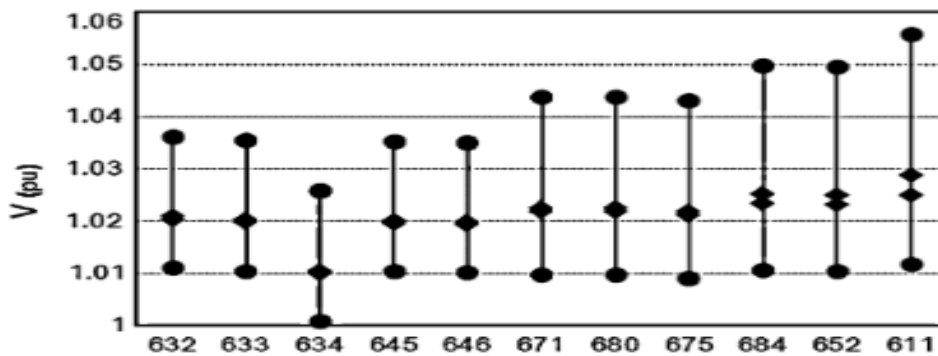


Fig. 9. Maximum and minimum values of bus voltages in the grid connected mode under light load conditions. DFIG reactive power regulated by PCM:,and unity power factor operation

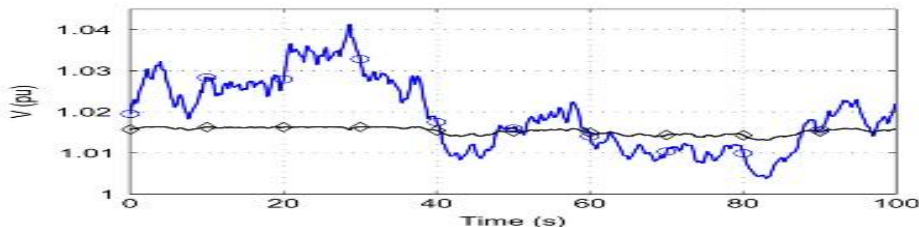


Fig. 10. Voltage at sensitive bus (652)in the grid connected mode under normal load conditions. DFIG reactive power regulated by PCM:,

Unity power factor operation is considered. The minimum and maximum voltages experienced at each bus with different wind speed series under this condition are shown in Fig. 9. The method decreases the voltage variation at bus 652 from 3.91% at UPF to 0.18%. Also, the method effectively reduces the voltage variations on the other buses. It should be noted that under the light load condition of microgrid, the transformer tap changer placed between bus 650 and bus 632 changes the tap to a 2.5% lower tap to maintain the voltage at bus 632.

Static Var Compensator is shunt connected type FACTS device which output is adjusted to exchange capacitive or inductive current and is used to maintain reactive power in network. And SVC contains two main components. Thyristor controlled/switched reactor (TSR) and switched capacitor

B. Medium Load Condition of Microgrid

Voltage variations of bus 652 under medium load conditions of the micro grid are displayed in Fig. 10 when the wind speed shown in Fig. 3 is considered. Sensitivity factors are calculated for the medium load condition; therefore, not surprisingly, control performance is excellent in decreasing voltage variations of bus 652 from 4.52% in UPF to 0.48%. Also the method reduces

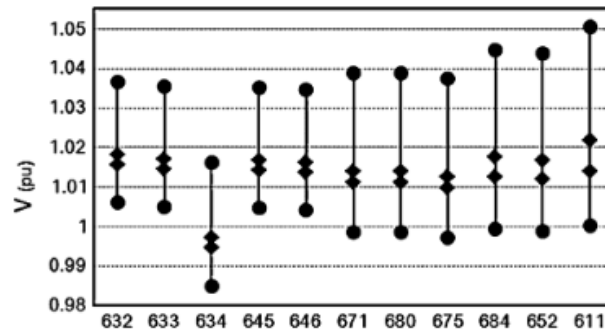


Fig. 11. Maximum and minimum values of bus voltages in the grid connected mode under normal load conditions. DFIG reactive power regulated by PCM:, and unity power factor operation

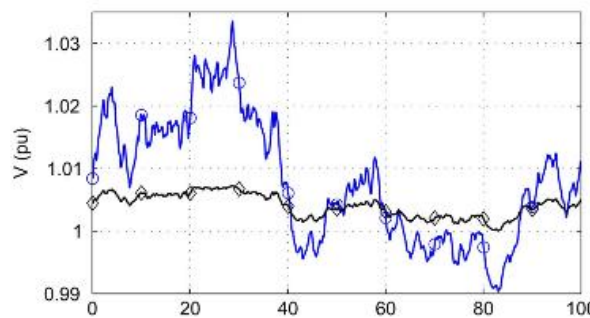


Fig. 12. Voltage at sensitive bus (652) in the grid connected mode under heavy load conditions. DFIG reactive power regulated by PCM:, and unity power factor operation

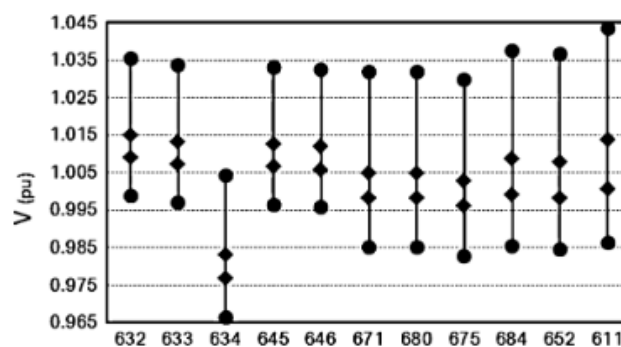


Fig. 13. Maximum and minimum values of bus voltages in the grid connected mode under heavy load conditions. DFIG reactive power regulated by PCM:, and unity power factor operation

B. Heavy Load Condition of Microgrid

Fig. 12 displays voltage variations of bus 652 under the heavy load condition of the micro grid when the wind speed shown in Fig. 3 is considered. The maximum and minimum of the voltages experienced at each of the microgrid buses are shown in Fig. 13. The proposed method decreases bus 652 voltage variations from 5.20% in the UPF to 0.95%. Also the method effectively reduces voltage

variations of other buses as shown in Fig. 13. It should be noted that under this load condition, the tap changer of the transformer place between bus 650 and bus 632 Changes the tap to a 2.5% higher tap to maintain the voltage at bus 632

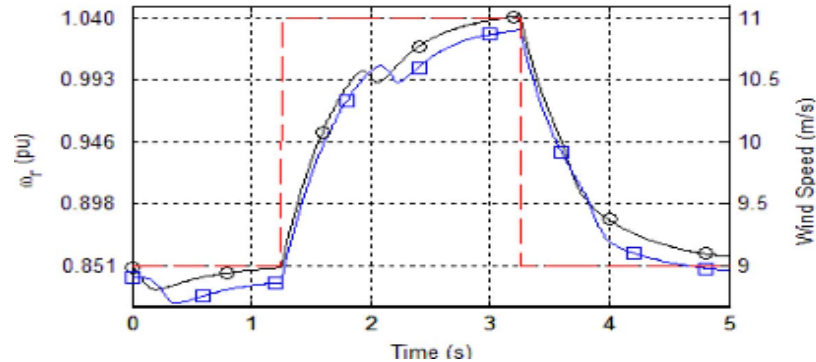


Fig. 14. Turbine speed with exact system parameters and 10% error in generator inductances for applied stepwise wind speed (dashed)

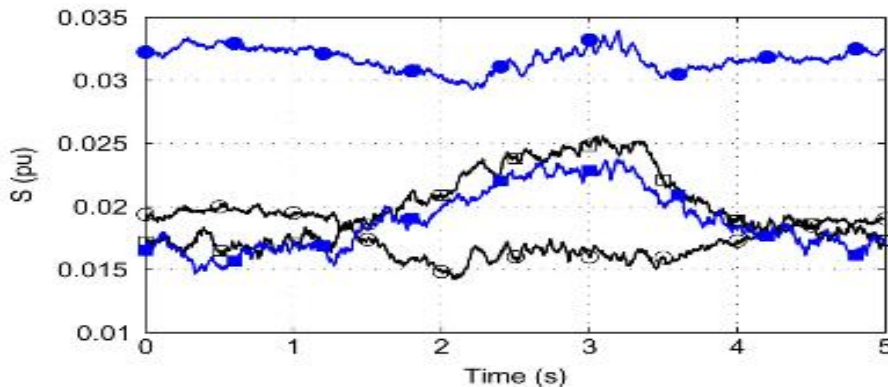


Fig. 15. Active and reactive power sliding variables with exact system parameters (notfilled) and 10% error in generator inductances (solidfilled)

D. System Robustness Evaluation

System disturbances and uncertainties are considered as in (11) in the controller design and the system should tolerate them providing their maximum values are less than. The maximum values of disturbances and uncertainties are considered equal to 10% of their relevant nominal state derivations. As a step-increase/decrease in wind speed as shown in Fig. 14 is applied to the wind turbine and simulations are carried out for two types of DFIG parameters of a) exact DFIG parameters, and b) 10% error in DFIG inductances. Figs. 14 and 15 display the turbine speed and sliding mode variables for the considered DFIG parameters. The mean values of active and reactive power sliding variables with exact DFIG parameters are 0.0175 and 0.02 pu, respectively. These values with the 10% error in DFIG inductances are 0.0317 and 0.0189 pu, respectively. It should be noted that the dips of turbine speed in Fig. 14 are the effect of the shadow phenomenon as periodical dips

CONCLUSION

The stochastic nature of wind can lead to significant voltage variations in micro grids. Based on voltage sensitivity analysis, this paper proposes a reactive power control method which can regulate the voltage at one or a group of the target buses in a micro grid while ensuring MPPT. The proposed method employs a sliding mode control scheme and directly controls the active and reactive powers of a DFIG wind system without involving any synchronous coordinate transformation. The method eliminates the need for decoupled proportional-integral (PI) loops; additionally, the control

performance is not degraded by errors in system parameters. Simulations show that the proposed control methods are effective at restricting the voltage swings experienced at different buses compared to the UPF method. The results are consistent for different loading conditions (low, medium, high) across different buses in the system. Compared to the UPF method, the average improvement in voltage regulation is noted to be 4.01% when considered across the three loading conditions. Also disturbances and uncertainties are effectively tolerated by the control system during the simulations. The proposed methodology can be potentially useful to robust reactive power management and voltage regulation in micro grids.

APPENDIX

TABLE II
PARAMETERS OF THE SIMULATED DFIG AND WIND TURBINE

R_s	0.03^{pu}	α	0.3
R_r	0.024^{pu}	R	42^m
X_s	$3.6 + 0.11^{pu}$	h	80^m
X_r	$3.6 + 0.102^{pu}$	a	2.5^m
X_m	3.6^{pu}	x	4.5^m
H	3.2	C_f	0.73
γ_1, γ_2	5		

REFERENCES

- [1] F. Katiraei, R. Iravani, N. Hatziargyriou, and A. Dimeas, "Microgridsmanagement," IEEE Power Energy Mag., vol.6, no.3 p.5465, May/June. 2008.
- [2] T.Sun,Z.Chen,and F.Blaabjerg,"Flicker study on variable speed wind turbines with doubly fed induction generators,"IEEE Trans. En-ergy Convers., vol. 20, no. 4, pp.896–905, Dec. 2005.
- [3] Y. S. Kim and D. J. Won, "Mitigation of the flicker level of a DFI Gusing power factor angle control,"IEEE Trans. Power Del.,vol.24,no. 4, pp. 2457–2458, Oct. 2009.
- [4] T. Thiringer, "Frequency scanning for power system property determination—Applied to a wind power grid,"IEEE Trans. Power Syst., vol.21, no. 2, pp. 702–708, May 2006.
- [5] A. Larsson, "Flicker emission of wind turbines during continuous operation,"IEEE Trans. Energy Converse., vol. 17, no. 1, pp. 114–118, Mar. 2002.
- [6] Standard for Interconnecting Distributed Resources With Electric Power Systems, IEEE 1547-2-2008, Dec. 2008.
- [7] R. Aghatehrani and R. Kavasseri, "Reactive power management of a DFIG wind system in micro grids based on voltage sensitivity analysis,"IEEE Trans. Sustain. Energy, vol. 2, no. 4, pp. 451–458, Oct. 2011.
- [8] L. Xu and P. Cartwright, "Direct active and reactive power control ofDFIG for wind energy generation,"IEEE Tran. Energy Convers., vol.21, no. 3, pp. 750–758, Sep.2006.
- [9] S. Z. Chen, N. C. Cheung, K. C.Woong, and J. Wu, "Integral sliding-mode direct torque control of doubly-fed induction generators under unbalanced grid voltage,"IEEE Trans. Energy Convers., vol. 25, no.2, pp. 356–367, Jun. 2010.
- [10] C. Lascu, I. Boldea, and F. Blaabjerg, "Very low speed variable structure control of sensorless induction machine drives without signal injection,"IEEE Trans. Ind. Electron., vol. 41, no. 2, pp. 591–598, Mar.2005.
- [11] K. P. Gokhale, D. W. Karraker, and S. J. Heikkila, "Controller for around Rotor Slip Ring Induction Machine," U.S. Patent 6448735B1, Sep. 2002.
- [12] I. Munteanu, S. Bacha, A.Bratcu, J. Guiraud, and D. Roye, "Energy-reliability optimization of wind energy conversion systems by sliding mode control,"IEEE Trans. Energy Convers.,vol.23,no.3,pp. 975–985, Sep. 2008
- [13] B. Beltran, T. Ali, and M. Benbouzid, "Sliding mode power control of variable speed wind energy conversion systems,"IEEE Trans. Energy Convers., vol. 23, no. 2, pp. 551558, Jun. 2008.

- [14] J. Hu, H. Nian, B. Hu, Y. He, and Z. Zhu, "Direct active and reactive power regulation of DFIG using sliding-mode control approach," *IEEE Trans. Energy Convers.* vol. 25, no. 4, pp. 1028–1039, Dec. 2010.
- [15] F. Valenciaga and P. F. Puleston, "Variable structure control of a wind energy conversion system based on a brushless doubly fed reluctance generator," *IEEE Trans. Energy Convers.*, vol. 22, no. 2, pp. 499–506, Jun. 2007.
- [16] S. Elghali, M. Benbouzid, T. Ahmed-Ali, and J. Charpentier, "High-order sliding mode control of a marine current turbine driven doubly fed induction generator," *IEEE J. Ocean. Eng.*, vol. 35, no. 2, pp. 402–411, Apr. 2010.
- [17] W. H. Kersting, "Radial distribution test feeders," *IEEE Trans. Power Syst.*, vol. 6, no. 3, pp. 975–985, Aug. 1991.
- [18] N. Kelley and B. Jonkman, *Turbsim User's Guide* National Renewable Energy Laboratory (NREL), Golden, CO, Sep. 2008 [Online]. Available: <http://wind.nrel.gov/designcodes/preprocessors/turbsim/>
- [19] R. Fadaeinedjad, M. Moallem, and G. Moschopoulos, "Simulation of a wind turbine with doubly fed induction generator by FAST and simulink," *IEEE Trans. Energy Convers.*, vol. 23, no. 2, pp. 690–700, Jun. 2008.
- [20] J. Jonkman, *FAST User's Guide* National Renewable Energy Laboratory (NREL), Golden, CO, Mar. 2010 [Online]. Available: <http://wind.nrel.gov/designcodes/simulators/fast/>
- [21] J. M. Kennedy, B. Fox, T. Littler, and D. Flynn, "Validation of fixed speed induction generator models for inertial response using windfarm measurements," *IEEE Trans. Power Syst.*, vol. 26, no. 3, pp. 1454–1461, Aug. 2011.
- [22] D. S. L. Dolan and P. W. Lehn, "Simulation model of wind turbine torque oscillations due to wind shear and tower shadow," *IEEE Trans. Energy Convers.*, vol. 21, no. 3, pp. 717–724, Sep. 2006.
- [23] H. K. Khalil, "Nonlinear design tools," in *Nonlinear Systems*, 3rd ed. Upper Saddle River, NJ: Prentice-Hall, 2001, pp. 551–625.
- [24] V. I. Utkin, "Sliding mode control design principles and applications to electric drives," *IEEE Trans. Ind. Electron.*, vol. 40, no. 1, pp. 23–26, Feb. 1993.
- [25] A. F. Filippov, *Differential Equations With Discontinuous Right Hand Sides*. Dordrecht, The Netherlands: Academic, 1988.
- [26] W. Gao and J. C. Hung, "Variable structure control of nonlinear systems: A new approach," *IEEE Trans. Ind. Electron.*, vol. 40, no. 1, pp. 45–55, Feb. 1993.
- [27] J. Y. Hung, W. Gao, and J. C. Hung, "Variable structure control: A survey," *IEEE Trans. Ind. Electron.*, vol. 40, no. 1, pp. 2–22, Feb. 1993.